

Sharpening of Neurite Morphology using Complex Coherence Enhanced Diffusion

Izadora Mustaffa, Carlos Trenado, Hazli Rafis Abd. Rahim, Karl-Herbert Schäfer and Daniel J. Strauss

Abstract—The study of the molecular mechanisms involved in neurite outgrowth and differentiation, requires essential accurate and reproducible segmentation and quantification of neuronal processes. The common method used in this study is to detect and trace individual neurites, i.e. neurite tracing. The challenge comes mainly from the morphological problem in which these images contains ambiguities such as neurites discontinuities and intensity differences. In our work, we encounter a bigger challenge as the neurites in our images have a higher density of neurites. In this paper, we present a hybrid complex coherence-enhanced method for sharpening the morphology of neurons from such images. Coherence-enhanced diffusion (CED) is used to enhance the flowlike structures of the neurites, while the imaginary part of the complex nonlinear diffusion of the image cancels the appearance of 'clouds'. We also describe an elementary method for estimating the density of neuritis based on the obtained images. Our preliminary results show that the proposed methodology is a step ahead toward an effective neuronal morphology algorithm.

I. INTRODUCTION

The study of neurite growth is fascinating for obvious reasons. It helps us to understand the most fundamental 'wirings' of the human body. It also helps us to understand various neurodegenerative diseases, such as Alzheimer's disease. Several methods to detect and trace neurites individually have been proposed based on vectorial tracking [1], chromosomes tracing [2], retinal vasculature [3] and multiscale feature analysis [4]. Before further analysis could be done on the neurites images, firstly, we need to overcome the ambiguities of the neurites images, i.e. neurites discontinuities, neurites with difference intensity levels and 'clouds' which appear in a closely clustered neurites, refer to Fig. 1. In the case of segmentation of the flow-like structures, i.e. neurites discontinuities, proves to be a challenge. Some images are of poor quality, such that it becomes necessary to enhance indistinct and/or close interrupted lines [5].

In cellular biology the problem arises, for example, when studying the axonal and dendritic outgrowth of cortical neurons under the influence of different promoting and inhibiting factors. Since a cell in culture grows approximately in a single cell layer, these process are usually studied by means of fluorescence microscopy. The images frequently contain ambiguities regarding the branching or crossing of neurites and the linking of fragmented neurite segments.

I. Mustaffa, C. Trenado and D.J. Strauss are with the Computational Diagnostics and Biocybernetics Unit at Saarland University and Saarland University of Applied Sciences, Homburg/Saarbruecken, Germany. Karl-Herbert Schäfer is with the University of Applied Sciences Kaiserslautern. {izadora,trenado,strauss}@cdb-unit.de. D. J. Strauss and C. Trenado are also with the Leibniz-Institute for New Materials, and D. J. Strauss with Key Numerics, Saarbruecken, Germany.

Such deficiencies make it virtually impossible to develop fully automatic tracing techniques for neurite tracing. This is why biologist still resort to manual delineation which is a time consuming process resulting in highly operator-dependent segmentation [6]. Most of the work done in regards of analyzing neurites images are done on images with low density of neurites [7], [8] or only focusing on the neurons [9]. Intense work are being carried out in modeling the morphology of neurite outgrowth [10], [11]. For our research however, the density of neurites in an image is of interest. Hence, a pseudo-quantification of neurite density is suggested.

In this paper we present a synthesis of two diffusion techniques proposed by [5] and [12], i.e. coherence-enhanced diffusion (CED) and complex nonlinear diffusion (CNLD).

II. MATERIAL AND METHODS

A. Neurite Image

The image of the neurites are of neurite networks created by isolating and dissociating dorsal root ganglia from newborn rats. Neurones were grown for up to 5 days and stained for the neuronal marker Tubulin using a green secondary fluorescence labeled antibody. The image was captured using Olympus IX-70 fluorescence microscope.

Fig. 1 shows a high neurite density image. In this figure, ambiguities of neurite image are shown. The RGB image processed using the CED to enhance its flow-like structures. CNLD is then applied to visibly enhance the structures before the density estimation is calculated.

B. Coherence-Enhanced Diffusion

Nonlinear diffusion filters which improves images with flow-like structures have been discussed extensively in [13] and have been further developed using vector-valued images and presented in [5]. The structure tensor is applied in the diffusion process because it allows both orientation estimation and image structure analysis. While most nonlinear diffusion process works on edge preserving ([14], [15]), the CED employs an integration scale which ensures stable orientation estimates and utilizing the difference of the eigenvalues of the structure tensor as a coherence measure. The anisotropic diffusion filtering make use of the information applying them to the structure tensor.

In the non-vector valued image, the idea is that the processed version of the image $u(x, t)$ of an image $f(x)$ with a scale parameter $t \geq 0$ as the solution of a diffusion equation

$$\partial_t u = \text{div}(D \cdot \nabla u) \quad (1)$$

with f as initial condition,

$$u(x, 0) = f(x) \quad (2)$$

and reflecting the boundary conditions:

$$\langle D\nabla u, n \rangle = 0 \quad (3)$$

Hereby the n denotes the outer normal and \langle, \rangle the usual Euclidean scalar product.

The diffusion tensor D which is a definite 2×2 matrix, steers the the diffusion process according to its eigenvalues (how much diffusivity) and eigenvector (directions of the diffusivity). The diffusion tensor is adapted to the evolving image.

A common diffusion tensor for all channels is being used to avoid the risk that a structure evolves at different locations for different channels. The vector-valued diffusion filter has the following structure ($i = 1, \dots, m$),

$$\partial_t u_i = \operatorname{div}(D \cdot \nabla u_i) \quad (4)$$

$$u_i(x, 0) = f_i(x) \quad (5)$$

$$\langle D\nabla u_i, n \rangle = 0 \quad (6)$$

Since D should take into account information from all channels, a natural choice would be to make it a function of $J_\rho(\nabla u_\sigma)$, the structure tensor for vector images. For enhancing coherence, the smoothing process should act along the coherence direction and increase with coherence. D should possess the same eigenvectors as the structure tensor. The eigenvalues of D are chosen as

$$\lambda_1 := \alpha \quad (7)$$

$$\lambda_2 := \begin{cases} \alpha, & \text{if } \mu_1 = \mu_2, \\ \alpha + (1 - \alpha) \exp\frac{-C}{(\mu_1 - \mu_2)^2}, & \text{else.} \end{cases} \quad (8)$$

with the threshold parameter, $C > 0$ and a small regularization parameter, $\alpha \in (0, 1)$. λ_2 is an increasing function with respect to the coherence $(\mu_1 - \mu_2)^2$. For a more detailed explanation regarding analyzing the coherence, parameter determination and selection, please refer to [5].

C. Complex Nonlinear Diffusion

This is a diffusion process with complex valued diffusion coefficient for modeling the blurring process. It was inspired by the free *Schrödinger* equations and is a generalization of the real diffusion process. For small phase angles, the linear process generates the Gaussian and Laplacian pyramids (scale-spaces) simultaneously. This approach has subsequently been widely used in low level vision tasks like smoothing, segmentation and edge detection [12]. To avoid confusion, for this section, image is denote as I .

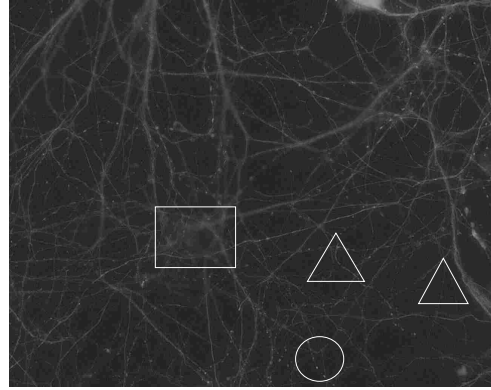


Fig. 1. Ambiguities in neurite image. \circ Neurite discontinuities, Δ Neurites with different intensities and \square 'Clouds' appearing in a cluster of neurites

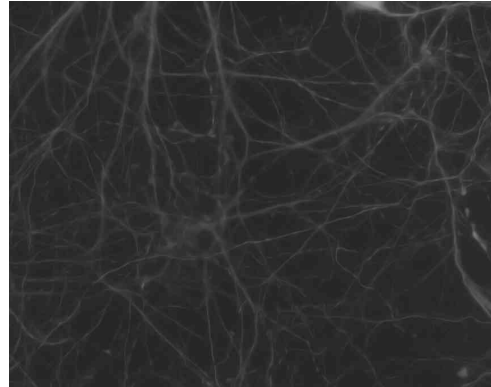


Fig. 2. Image after coherence-enhanced diffusion

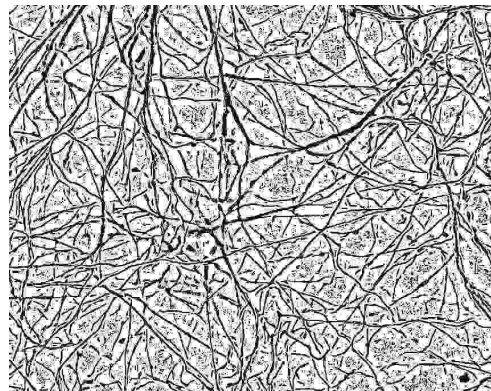


Fig. 3. Binary image of the imaginary part of the complex nonlinear diffusion.

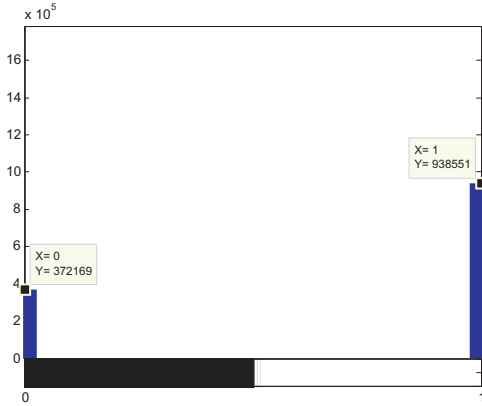


Fig. 4. Histogram of the binary image. The black pixels represents the foreground which is the neurites and the white pixels is the background. The size of the image is 1024x1280 pixels, ratio of foreground to the background is 28.39%

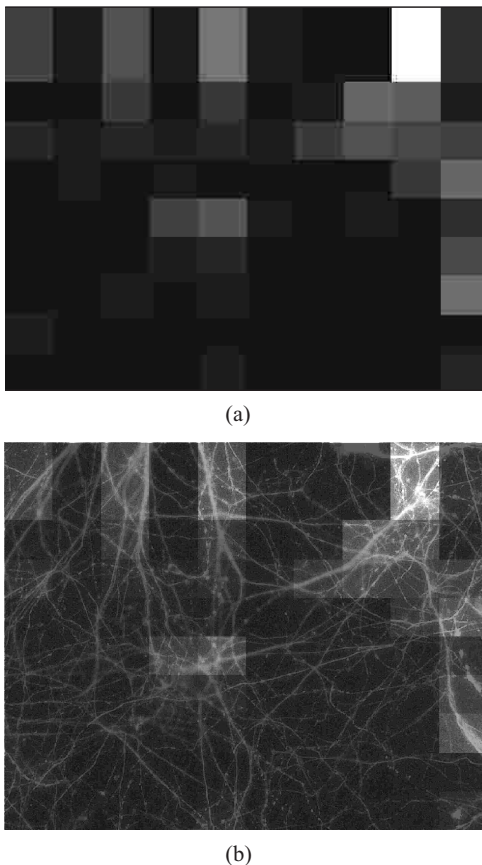


Fig. 5. Spatial density of the neurites. (a) The grayscale of neurite image after CED is divided into a 10x10 grid. Each grid shows a histogram count on the higher end of the grayscale. (b) The spatial density map is superimposed on the grayscale image of the neurites to locate which area has a higher density than the other.

The the one dimensional case, linear scale–space equation is given by:

$$I_t = c\Delta I, \quad I|_{t=0} = I_0, \quad 0 < c \in \mathbb{R} \quad (9)$$

with a constant diffusion coefficient $c = 1$.

The following initial value problem is considered:

$$\begin{aligned} I_t &= cI_{xx}, & t > 0, & \quad x \in \mathbb{R} \\ I(x, 0) &= I_0 \in \mathbb{R}, & c, I \in \mathbb{C} \end{aligned} \quad (10)$$

When $c \in \mathbb{R}$ there are two cases: for $c > 0$ the process constitutes a well-posed forward diffusion, whereas for $c < 0$ an ill-posed inverse diffusion process is obtained. In the general case the initial condition I_0 is complex. In this paper we discuss the particular case of real initial conditions, where I_0 is the original image.

In regard of (10), the complex fundamental solution $h(x, t)$ that satisfies the relation below is sought:

$$I(x, t) = I_0 * h(x, t) \quad (11)$$

where $*$ denotes convolution. Letting the c coefficient in (10) be $c = re^{i\theta}$, since there does not exist a stable fundamental solution of the inverse diffusion process, restrict the analysis to a positive real value of c , that is $\theta \in (-\frac{\pi}{2}, \frac{\pi}{2})$. Replacing the real time variable t by the complex time $\tau = ct$, yields $I_\tau = I_{xx}$, $I(x, 0) = I_0$. This is identical in its form to the linear real-valued diffusion equation. Its fundamental solution, therefore, is in a Gaussian form. In order to satisfy the initial condition $I(x, 0) = I_0$ we require

$$\begin{aligned} (a) \quad & \int_{-\infty}^{\infty} h(x, t \rightarrow 0) dx = 1, \\ (b) \quad & \int_{|x| > \epsilon} |h(x, t \rightarrow 0)| dx \rightarrow 0, \end{aligned} \quad (12)$$

where $\epsilon = \epsilon(t)$, $\lim_{t \rightarrow 0} \epsilon(t) = 0$.

This leads to the following fundamental solution:

$$h(x, t) = A g_{\sigma(t)}(x, t) e^{i\alpha(x, t)}, \quad (13)$$

where $g_{\sigma}(x, t) = \frac{1}{\sqrt{2\pi\sigma(t)}} e^{-x^2/2\sigma^2(t)}$, and

$$A = \frac{1}{\sqrt{\cos \theta}}, \quad \alpha(x, t) = \frac{x^2 \sin \theta}{4tr} - \frac{\theta}{2}, \quad \sigma(t) = \sqrt{\frac{2tr}{\cos \theta}} \quad (14)$$

The changing values of theta can make a big impact on the image processed with complex diffusion. As the theta value increases, the image will sharpen more (sharpening property increases) till the theta value reaches 180 degree, and the sharpening property reduces (smoothing property increases) from 181 to 360 degrees and the process continues. Please refer to [16] for a more detailed explanation. The value of theta used in this paper is as suggested by the author in [12].

III. RESULT AND DISCUSSION

The described techniques were implemented using a technical computing software from Mathworks, USA. Only one neurite image is presented here to demonstrate the workings of the proposed method. The result of the CED is shown in Fig. 2. The flow-like structures of the neurites with lesser intensity level are enhanced and most neurites discontinuities are also recovered.

From this image we made a spatial density map of the neurites. A grayscale image of the CED image is divided into 10x10 grid. For each grid, we calculate the number of pixels located in the higher end of the gray scale. To facilitate the visual comparison between the grayscale image and the spatial density map, we have superimposed the image together as seen in Fig.5. The lighter the color is, the higher the density of the neurites are in the specific grid. Next, we applied the CNLD, which yields a real and imaginary part of the CED image. The imaginary part is our main interest as it only shows the edges of the neurites. We convert the imaginary part of the image into a binary image. From here, fine structures which were hardly seen visually in the real part of the CED image are visually clear, and 'clouds' are removed, revealing hidden neurites underneath it, refer Fig.3. The density estimation of the neurites is shown by Fig.4. Through the histogram of the binary neurite image we are able to calculate the ratio between the neurites (black pixels) and background (white pixels) and make an estimation of neurites density.

We acknowledge that in enhancing and recovering the flow-like structures, not all neurites discontinuities could be recovered. This task could be achieved with a longer CED process, however, on the expense of losing several fine structures. Hence a compromise has to be made in choosing the diffusion time. We also observe the level of intensity increases in both neurites with low and high intensities. The latter however is not desired. We also acknowledge the presence of background structures which appears in between encircling neurites which is visible in the binary image of the complex neurite image. This naturally also affects the density estimation in the histogram. This is also the reason why the spatial density map was not based on the binary image rather on the gray scale CED image.

IV. CONCLUSIONS AND FUTURE WORKS

This paper has shown a novel application of the hybrid complex coherence-enhanced method in sharpening and enhanced neurites morphology. We have shown that using the CED, the image which contains a dense flow-like structures and are closely located is enhanced. While incorporating the CNLD, the edges of the structures are more visible. We also presented a prefatory method to quantify the density of the neurites objectively and spatially.

Further work is undergoing in equalizing the intensity of the neurites and removing the background structures affecting the estimation density calculation. Parameters used in this method need to be further explored to make it accustomed to neurite images and more robust. Overcoming these

drawbacks would not only produce a conclusive estimation of the neurite density but also a neurite image with an enhanced neurite morphology.

V. ACKNOWLEDGMENTS

Izadora Mustaffa and Hazli Rafis Abd. Rahim are supported by Universiti Teknikal Malaysia Melaka, the Ministry of High Education of Malaysia and the German Federal Ministry of Education and Research (BMBF), Grant FZ: 17N1208.

REFERENCES

- [1] K. Al-Kofahi, S. Lasek, D. Szarowski, C. Pace, G. Nagy, J. Turner, and B. Roysam, "Rapid automated three-dimensional tracing of neurons from confocal image stacks," *IEEE Transactions on Information Technology in Biomedicine*, vol. 6, pp. 171–187, 2002.
- [2] A. Houtsmuller, A. Smeulders, H. van der Voort, J. Oud, and N. Nanninga, "The homing cursor: A tool for three-dimensional chromosome analysis," *Cytometry*, vol. 14, pp. 501–509, 1993.
- [3] A. Can, H. Shen, J. N. Turner, H. L. Tanenbaum, and B. Roysam, "Rapid automated tracing and feature extraction from retinal fundus images using direct exploratory algorithms," *IEEE Transaction on Information Technology in Biomedicine*, vol. 3, pp. 125–138, 1999.
- [4] A. Dima, M. Scholz, and K. Obermayer, "Automatic segmentation and skeletonization of neurons from confocal microscopy images based on the 3-d wavelet transform," *IEEE Trans. Image Proc.*, vol. 11, pp. 790–801, 2002.
- [5] J. Weickert, "Coherence-enhancing diffusion of colour images," *Image and Vision Computing*, vol. 17, pp. 201–212, 1999.
- [6] E. Meijering, M. Jacob, J.-C. Sarria, and M. Unser, "A novel approach to neurite tracing in fluorescence microscopy images," in *Proceedings of the Fifth IASTED International Conference on Signal and Image Processing (SIP'03)*, M. H. Hamza, Ed. ACTA Press, Calgary., 2003, pp. 491–495.
- [7] E. Meijering, M. Jacob, J.-C. Sarria, P. Steiner, H. Hirling, and M. Unser, "Design and validation of a tool for neurite tracing and analysis in fluorescence microscopy images," *Cytometry Part A*, vol. 58A, no. 2, pp. 167–176, April 2004.
- [8] D. Yu, D. T. Pham, H. Yan, B. Zhang, and D. I. Crane, "Segmentation of cultured neurons using logical analysis of grey and distance difference," *Journal of Neuroscience Methods*, vol. 166, pp. 125–137, 2007.
- [9] I. Kim, H. N. Beck, P. J. Lein, and D. Higgins, "Interferon gamma induces retrograde dendritic retraction and inhibits synapse formation," *Journal of Neuroscience*, vol. 11, pp. 4530–4539, 2002.
- [10] B. P. Graham and A. Van Ooyen, "Mathematical modelling and numerical simulation of the morphological development of neurons," *BMC Neuroscience*, vol. 7, 2006.
- [11] G. Kiddie, D. McLean, A. Van Ooyen, and B. Graham, "Biologically plausible models of neurite outgrowth," *Progress in Brain Research*, vol. 147, pp. 67–80, 2005.
- [12] G. Gilboa, N. Sochen, and Y. Y. Zeevi, "Image enhancement and denoising by complex diffusion processes," *IEEE Transactions On Pattern Analysis And Machine Intelligence*, 2003.
- [13] J. Weickert, *Anisotropic Diffusion in Image Processing*, 1996.
- [14] A. Chambolle, "Partial differential equations and image processing," in *Proc. IEEE Int. Conf. Image Processing*, vol. 1. IEEE Computer Society Press, Nov 1994, pp. 16–20.
- [15] G. Sapiro and D. Ringbach, "Anisotropic diffusion of multivalued images with applicationsto color filtering," *IEEE Trans. Image Proc.*, vol. 5, pp. 1582–1586, November 1996.
- [16] G. Gilboa, "Super-resolution algorithms based on inverse diffusion-type processes," Ph.D. dissertation, Technion-Israel Institute of Technology, March 2004.